Two-phonon structure of low-energy 1^+ excitations of ^{130}In

A. P. Severyukhin,[1,2] N. N. Arsenyev,[1] I. N. Borzov,[3,1] E. O. Sushenok,[1] D. Testov,[1,4] and D. Verney[5]
[1] *Joint Institute for Nuclear Research, 141980 Dubna, Moscow region, Russia*
[2] *Dubna State University, Universitetskaya street 19, 141982 Dubna, Moscow region, Russia*
[3] *National Research Centre "Kurchatov Institute," 123182 Moscow, Russia*
[4] *Dipartimento di Fisica e Astronomia and INFN, Sezione di Padova, Padova, Italy*
[5] *Université Paris-Saclay, CNRS/IN2P3, IJCLab, 91405 Orsay, France*

(Received 31 March 2019; revised manuscript received 29 February 2020; accepted 22 April 2020; published 12 May 2020)

The 1^+ spectrum of ^{130}In populated in the β decay of ^{130}Cd is studied. The coupling between one- and two-phonon terms in the wave functions of 1^+ states is taken into account within the microscopic model based on the Skyrme interaction. The approach enables one to perform the calculations in very large configurational spaces. The new calculation is extended by enlarging the variational space for the 1^+ states with the inclusion of the two-phonon configurations. The dominant contribution to the additional 1^+ states comes from the $[3^+ \otimes 2^+]_{\rm QRPA}$ two-phonon configurations constructed from the charge-exchange 3^+ phonons. A correlation is found between the low-lying $E2$ transition strengths of the parent and daughter isobaric companions. Using the same set of parameters this correlation is studied also for ^{126,128}In and ^{126,128}Cd.

DOI: 10.1103/PhysRevC.101.054309

I. INTRODUCTION

The hypothetical paths of astrophysical r-process nucleosynthesis within the nuclear chart run through very-neutron-rich nuclei far off the stability. The β-decay properties of canonical waiting-point nuclei in the vicinity of the neutron $N = 82$ shell play an important role in defining the r-process timescale for the matter flow from the r-process seed to superheavy nuclei. The half-lives $T_{1/2}$ and delayed multineutron emission probabilities directly influence the shape of the second abundance peak at its rising wing. Recent experiments at RIKEN high-current cyclotrons [1] using the β-γ coincidence technique have provided β-decay half-lives for many r-process nuclei which impact the abundance calculations. In particular, the half-life of $T_{1/2} = 127(2)$ ms measured for ^{130}Cd in Ref. [1] turns out to be shorter than that previously reported in Refs. [2–4]. This fact may not only affect current r-process modeling but also provide an additional piece of information for solving the long-standing ^{130}Cd β-decay puzzle.

It has been well known that the β decay of ^{130}Cd is dominated by the Gamow-Teller (GT) transition to the first 1^+ state at the excitation energy of 2120 keV in the daughter odd-odd nucleus ^{130}In [4]. The puzzle has appeared when the state-of-the-art shell-model calculations underestimated the energy of this state built on the simple $\{\pi 1g_{9/2}, \nu 1g_{7/2}\}$ configuration. Namely, in the calculations from Refs. [4,5], this state turned out to be lower by 550–750 keV than the experiment. To cure such a significant discrepancy, an empirical monopole term was introduced [6]. Another way to solve the puzzle was found in the so-called shell quenching associated with neutron skin formation [7].

However, the more recent mass and β-decay half-life measurements have shown rather robust $N = 82$ neutron shells [1]. Further progress has been achieved by using a renormalized CD-Bonn interaction within the $V_{{\rm low}\, q}$ framework [8] in more recent shell-model calculations extended to the neutron $(g - h)$, proton $(f - g)$ model space [9]. Even though, the experimental 1^+ state position turned out to be reachable only if a significant arbitrary renormalization is assumed of the proton-proton pairing, as well as neutron-neutron and neutron-proton (np) components of the leading shell-model configurations.

It is the aim of the present paper to investigate ^{130}Cd decay properties from the point of view of the quasiparticle random-phase approximation (QRPA), using a larger configuration space than available within the shell model and extending the variational space to include phonon-phonon coupling (PPC) effects. Such an approach may provide new insights on the structure involved. It has also several formal advantages: the Ikeda sum rule for GT transitions is naturally exhausted and no effective charge for the electric transition probability calculation is required. Furthermore, by using a Skyrme interaction with inclusion of tensor terms no quenching factor is required. In this framework, phonon-phonon couplings are expected to play a significant role in the neutron-rich Cd decays. Indeed, for the $^{124-132}$In isotopic chain, the ground-state spin-parities change from $J^\pi = 3^+$ in ^{128}In to $J^\pi = 1^-$ in ^{130}In in which the energy of the 3^+ state is 388.3(2) keV [10]. As shown in Refs. [11,12], the spin inversion impacts the β-decay properties producing a slower decrease or even a stabilization in mass dependence of the half-lives. The coupling with the charge-exchange 3^+ phonons may substantially enrich the low-energy 1^+ spectrum of the daughter nucleus.

 ©2020 American Physical Society

Furthermore, the fact that the spin-parity of the ^{130}In ground state turns out to be 1^- indicates that one may expect the coupling with the charge-exchange 1^- phonons also to contribute with small components in the phonon structures of the low-lying 1^+ states.

Two-phonon structures have a strong influence on electric transition probabilities. For even-even heavy vibrational nuclei, the lowest known 1^- states, come from the two-phonon structure composed of the quadrupole and octupole phonons. At the same time first one-phonon 1^- state in the calculations within the QRPA appears above 5 MeV [13,14]. As shown in Ref. [15], there is an empirical correlation between $B(E1; 1^-_1 \rightarrow 0^+_{\mathrm{g.s.}})$ and $B(E1; 3^-_1 \rightarrow 2^+_1)$ values. This low-energy $E1$ transition is forbidden in the ideal boson picture and has been calculated in the quasiparticle-phonon model (QPM) [16] taking into account the internal fermion structure of phonons [17,18].

As shown in Refs. [19,20] for the self-conjugate nuclei ($N = Z$), "the nuclear shell-model calculations show a clear anticorrelation between the GT strength and the transition rate of the collective quadrupole excitation from the ground state in response to artificial changes of the spin-orbit splitting." For the case of ^{130}In, the influence of the PPC on the 1^+_1 description has been analyzed within the microscopic model based on the QRPA with the Skyrme interaction in Ref. [21]. The $[2^+_1]_{\mathrm{QRPA}}$ state of the parent nucleus ^{130}Cd is the lowest collective excitation which leads to the minimal two-phonon energy and the maximal matrix elements for coupling of the one- and two-phonon configurations. Finally, as it is pointed out in Refs. [21,22], the $[1^+_1 \otimes 2^+_1]_{\mathrm{QRPA}}$ configuration is the important ingredient for the calculation of the half-life and the P_{2n}/P_{1n} ratio.

In the present work, calculation details are identical to Ref. [21]; however, the two-phonon basis coupled to $J^\pi = 1^+$ is constructed from the charge-exchange QRPA phonons with the following multipolarities:

$$\lambda^\pi = 1^+,\ 1^-,\ 2^-,\ 3^+, \tag{1}$$

and the vibrational QRPA phonons with the following multipolarities:

$$\lambda'^{\pi'} = 1^-,\ 2^+,\ 3^-,\ 4^+. \tag{2}$$

This means that the two-phonon configurational space is now enlarged by the phonon compositions $[\lambda^\pi \otimes \lambda'^{\pi'}]_{\mathrm{QRPA}}$, i.e., $[3^+ \otimes 2^+]_{\mathrm{QRPA}}$, $[3^+ \otimes 4^+]_{\mathrm{QRPA}}$, $[2^- \otimes 3^-]_{\mathrm{QRPA}}$, $[2^- \otimes 1^-]_{\mathrm{QRPA}}$, and $[1^- \otimes 1^-]_{\mathrm{QRPA}}$.

II. QUASIPARTICLE RANDOM-PHASE APPROXIMATION RESULTS

The wave functions are constructed from a linear combination of one- and two-phonon configurations as

$$\Psi_\nu(JM) = \left(\sum_i R_i(J\nu) Q^+_{JMi} + \sum_{\lambda_1 i_1 \lambda_2 i_2} P^{\lambda_1 i_1}_{\lambda_2 i_2}(J\nu) \left[Q^+_{\lambda_1 \mu_1 i_1} \bar{Q}^+_{\lambda_2 \mu_2 i_2} \right]_{JM} \right) |0\rangle, \tag{3}$$

where λ denotes the total angular momentum and μ is its z projection in the laboratory system. The ground state of ^{130}Cd is assumed to be the QRPA phonon vacuum $|\,0\rangle$.

The wave functions $Q^+_{\lambda\mu i}|0\rangle$ of the $[1^+_i]_{\mathrm{QRPA}}$, $[3^+_i]_{\mathrm{QRPA}}$, $[1^-_i]_{\mathrm{QRPA}}$, and $[2^-_i]_{\mathrm{QRPA}}$ states of ^{130}In are described as linear combinations of two-quasiparticle (2QP) neutron-proton configurations. The cutoff of the discretized continuous part of the single-particle spectra is performed at the energy of 100 MeV. This is sufficient for exhausting the Ikeda sum rule for GT transitions $S_- - S_+ = 3(N - Z)$. The finite-rank separable approximation [23–25] for the residual interactions facilitates the QRPA calculations in very large 2QP spaces. As the parameter set in the particle-hole (p-h) channel, we used the Skyrme interaction T43 with tensor components included [26]. The pairing correlations are generated by a zero-range surface force [21,27]. As proposed in Ref. [28], the $E_x(1^+_i)$ energies can be estimated by the following expression:

$$E_x(1^+_i) \approx E_i - \Omega, \tag{4}$$

where E_i are the $[1^+_i]_{\mathrm{QRPA}}$ eigenvalues of the QRPA equations and Ω corresponds to the lowest 2QP energy. The possible spin-parity of the lowest 2QP state $\{\pi 1g_{9/2}, \nu 1h_{11/2}\}$ is $J^\pi = 1^- - 10^-$. The QRPA analysis within the one-phonon approximation results in the spin-parity of the ground state, $J^\pi = 1^-$. In Eq. (4), a more precise value for Ω is used which is equal to the $[1^-_1]_{\mathrm{QRPA}}$ energy. The crucial contributions to the wave functions of the $[1^+_{1,2}]_{\mathrm{QRPA}}$ states with energies E_x, 3.6 and 5.6 MeV, come from the configurations $\{\pi 1g_{9/2}, \nu 1g_{7/2}\}$ and $\{\pi 2d_{5/2}, \nu 2d_{3/2}\}$, respectively. The dominant configuration of the $[3^+_1]_{\mathrm{QRPA}}$ state with $E_x = 1.1$ MeV is of $\{\pi 1g_{9/2}, \nu 2d_{3/2}\}$. It is seen that the $[3^+_1]_{\mathrm{QRPA}}$ energy is less than one-third of the $[1^+_1]_{\mathrm{QRPA}}$ energy.

$\bar{Q}^+_{\lambda\mu i}|0\rangle$ are dipole, quadrupole, octupole and hexadecapole QRPA vibrations of ^{130}Cd. The closure of the neutron subshell $1h_{11/2}$ in ^{130}Cd leads to the vanishing of the neutron pairing. As a result, the 2^+_1 (4^+_1) state with $E_x = 1.3$ MeV (1.6 MeV) has the $\{1g_{9/2}, 1g_{9/2}\}_\pi$ configuration dominating 96% (98%) and the $B(E2)$ [$B(E4)$] value is of 5.7 W.u (4.4 W.u.). Because of the large configurational space, we do not use effective charges. At the same time, the main part of the $E2$ strength exciting the 2^+_1 state is generated by the 2QP configurations of the giant quadrupole resonance (see Fig. 1). This effect has previously been observed in the case of ^{92}Zr [29]. For the 2^+_2 and 4^+_2 QRPA states with $E_x = 4.1$ and 4.6 MeV, the main components of the wave function are the configurations $\{2f_{7/2}, 1h_{11/2}\}_\nu$ and $\{2d_{5/2}, 1g_{9/2}\}_\pi$, which lead to the comparatively large values $B(E2; 2^+_2 \rightarrow 0^+_{\mathrm{g.s.}}) = 4.5$ W.u. and $B(E4; 4^+_2 \rightarrow 0^+_{\mathrm{g.s.}}) = 7.4$ W.u. The same configurations dominate in the structure of the 2^+_1 state of the doubly magic nucleus ^{132}Sn. It is worth pointing out that they are related to core-excited configurations in the shell-model calculation [9]. Because the data for the Cd isotopes are very scarce, the properties of the 2^+_1 state of ^{132}Sn [30] is used for reference. The value of 8.3 W.u. of the QRPA calculation [21] is overestimated by about 60%. One can expect an improvement if the two-phonon configurations are taken into account [31].

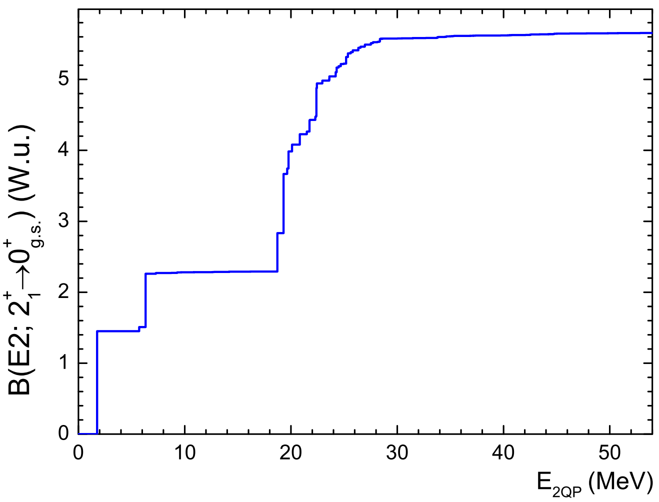

FIG. 1. Running sum of the $E2$-transition strength as a function of the 2QP energy included in the QRPA calculation for ^{130}Cd.

III. PHONON-PHONON COUPLING EFFECTS ON β-DECAY RATES

As in the QPM [16,32], the diagonalization of the Hamiltonian in the space of the one- and two-phonon configurations produces eigenvalues of 1^+_k states (E_k) [22,33]. The $E_x(1^+_k)$ energies are obtained by using the same ansatz (4). Because of the inclusion of the tensor correlation effects within the 1p-1h and 2p-2h configuration space, we do not need a quenching factor [34]. The β^--decay rate is expressed by summing up the probabilities (in units of $G_A^2/4\pi$) of the energetically allowed GT transitions [$E_x(1^+_k) < Q_\beta$] weighted with the integrated Fermi function f_0,

$$T_{1/2}^{-1} = \sum_k \lambda_{if}^k = D^{-1}\left(\frac{G_A}{G_V}\right)^2 \times \sum_k f_0(Z+1, A, Q_\beta - E_x(1^+_k))B(GT)_k, \quad (5)$$

where λ_{if}^k is the partial β-decay rate, $G_A/G_V = 1.25$ is the ratio of the weak axial-vector and vector coupling constants, and $D = 6147$ s (see Ref. [35]). For the case of the $N = 82$ isotone ^{130}Cd, one can neglect the first-forbidden (FF) β decays. According to Ref. [36], the contributions of the FF transitions to the half-life is 7.0%, and 11.755% in Ref. [37].

The partial β-decay rate has a strong energy dependence which approximately scales like $(Q_\beta - E_x)^5$. The partial β-decay rates calculated taking into account the two-phonon configurations $[\lambda^\pi \otimes \lambda'^{\pi'}]_{\rm QRPA}$ with the different

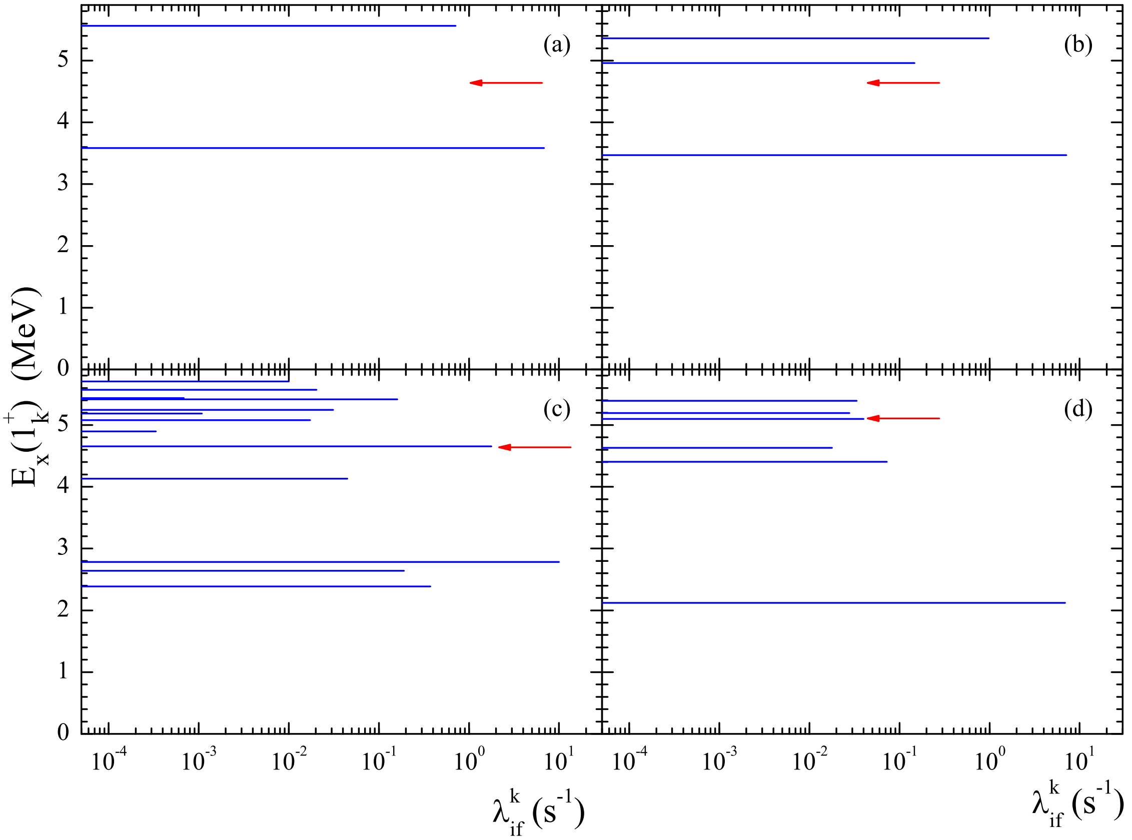

FIG. 2. β-transition rates in ^{130}Cd. (a), (b) Calculations within the QRPA and taking into account the $[1^+ \otimes 2^+]_{\rm QRPA}$ configurations [21], respectively. (c) Calculation taking into account the $[\lambda^\pi \otimes \lambda'^{\pi'}]_{\rm QRPA}$ configurations with the different multipolarities (1) and (2). (d) β-transition rates are taken from the analysis of the experimental data: Q_β and $E_x(1^+)$ energies, log ft values [9,10]. The calculated and experimental S_n energies [10] are denoted by the arrows in panels (a)–(d), respectively.

TABLE I. The calculated energies, log ft, transition probabilities, partial widths, and dominant components of phonon structures of the low-lying 1^+ states in ^{130}In.

				$1^+_k \to 1^-_{\rm g.s.}$		$1^+_k \to 2^-_1$		$1^+_k \to 3^+_1$	
1^+_k	Energy	Structure	log ft	$B(E1)$	$\Gamma(E1)$	$B(E1)$	$\Gamma(E1)$	$B(E2)$	$\Gamma(E2)$
	(MeV)			(W.u.)	(eV)	(W.u.)	(eV)	(W.u.)	(eV)
1^+_1	2.4	$99\%[3^+_1\otimes 2^+_1]$	4.7	4.2×10^{-7}	1.1×10^{-5}	4.5×10^{-6}	1.1×10^{-4}	5.8	7.2×10^{-4}
1^+_2	2.6	$97\%[3^+_1\otimes 4^+_1]$	4.9	5.3×10^{-7}	1.7×10^{-5}	0.7×10^{-6}	2.3×10^{-5}	0.1	2.6×10^{-5}
1^+_3	2.8	$77\%[1^+_1]$	3.1	0.9×10^{-5}	3.6×10^{-4}	1.2×10^{-5}	4.5×10^{-4}	0.1	4.8×10^{-5}
1^+_4	4.1	$92\%[2^-_1\otimes 3^-_1]$	4.8	1.5×10^{-5}	1.9×10^{-3}	2.2×10^{-5}	2.7×10^{-3}	0.1	8.2×10^{-4}
1^+_5	4.7	$57\%[1^+_2]+$ $32\%[3^+_1\otimes 2^+_2]$	2.8	0.7×10^{-5}	1.4×10^{-3}	2.0×10^{-4}	3.8×10^{-2}	1.0	2.0×10^{-2}

multipolarities (1) and (2) are given in Fig. 2(c). The half-life $T_{1/2} = 83$ ms is found. The results of the microscopic calculation are compared with the experimental data from Refs. [9,10] by using the following expression:

$$\lambda^k_{if} = f_0\big(Z+1, A, Q^{\rm expt}_\beta - E^{\rm expt}_x(1^+_k)\big)10^{-\log ft^{\rm expt}(1^+_k)}. \quad (6)$$

Using the partial β-decay rates obtained from Eq. (6), we estimate the half-life of 140 ms, which is close to the experimental value.

First, it is seen that the strength distribution is enriched compared with the pure QRPA one. Second, as it follows from Fig. 2 and Table I, the 1^+_1 and 1^+_2 states in our calculation have a prevailing two-phonon origin due to coupling of the 2^+_1 and 4^+_1 one-phonon excitations in the parent nucleus and the low-energy 3^+_1 excitation in its daughter. The strongest 1^+_3 state has a predominantly 2QP nature $\{\pi 1g_{9/2}, \nu 1g_{7/2}\}$. As one can see, the quantitative agreement with the experimental 1^+ energy of 2120 keV is not satisfactory. Thus, only a qualitative description of the experimental strength distribution (log $ft = 3.9 \pm 0.1$) [9] has been achieved. The inclusion of the four-quasiparticle configuration $\{\pi 1g_{9/2}, \pi 1g_{9/2}, \pi 1g_{9/2}, \nu 2d_{3/2}\}$ plays the key role in the calculations of the 1^+_1 and 1^+_2 states. Third, both calculated and experimental strength distributions have some strength concentration above the one-neutron emission threshold. The calculations reproduce satisfactory the centroid of this strength distribution. The 1^+_5 state with the β-transition rate of 1.8 s^{-1} is of mixed structure (see Table I). The main two-phonon component of the 1^+_5 wave function is the $[3^+_1 \otimes 2^+_2]_{\rm QRPA}$ configuration. In all calculated 1^+ states at excitation energies above 4.7 MeV, the β-transition rates with more than 0.02 s^{-1} originate from the two-phonon configurations composed of the 2^+_2 and 4^+_2 phonons. The present two-phonon space $[\lambda^\pi \otimes \lambda'^{\pi'}]_{\rm QRPA}$ incorporating the multipolarities (1) and (2) results in the substantial strength fragmentation compared with the calculation taking into account only the phonon composition $[1^+ \otimes 2^+]_{\rm QRPA}$ as proposed in Refs. [21,22]. It is worth mentioning that the first prediction of the core-excited configuration structure of the states above 3.5 MeV based on the shell-model calculation was done in Ref. [9].

We now turn to the level density and show in Fig. 3 the impact of the extension of the two-phonon space on the low-energy part of the spectrum $E_x(1^+_k)$. The results of the calculation taking into account the phonon composition $[1^+ \otimes 2^+]_{\rm QRPA}$ [21] indicate only three 1^+ states below 6 MeV. The inclusion of the rest of the two-phonon configurations leads to an increase of the level density and makes a downward shift of the low-energy spectrum $E_x(1^+_k)$. One can construct the staircase function $N(E)$ which is defined as the state number below the energy E. The staircase function of calculated 1^+ energies for ^{130}In is shown in Fig. 4. The function $N(E)$ can be described by the following level density:

$$\rho(E) = \alpha(E - E_0)^\beta. \quad (7)$$

We find that $E_0 = 0.43$ MeV, $\beta = 3.30$, and $\alpha = 2.6 \times 10^{-2}$ MeV$^{-\beta-1}$. Notice that, in the Fermi-gas model with equidistant single-particle spectrum, the exponent is $2n - 1$ for the density of np-nh excitations, and the value $\beta = 3$ for 2p-2h excitations, which is quite close to the fitted values of β.

IV. PHONON-PHONON COUPLING EFFECTS ON ELECTRIC TRANSITION PROBABILITIES

The quadrupole collectivity of the parent even-even nucleus makes the two-phonon states interesting and unique

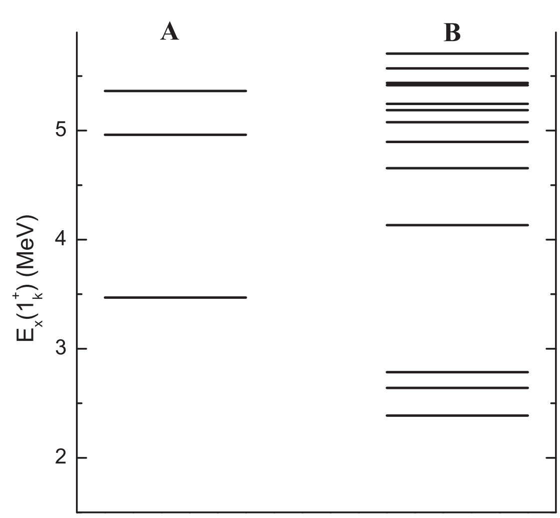

FIG. 3. Comparison of the low-energy 1^+ spectrum of ^{130}In calculated with the $[1^+ \otimes 2^+]_{\rm QRPA}$ configurations in Ref. [21] (column A) and with the full two-phonon basis for this work (column B).

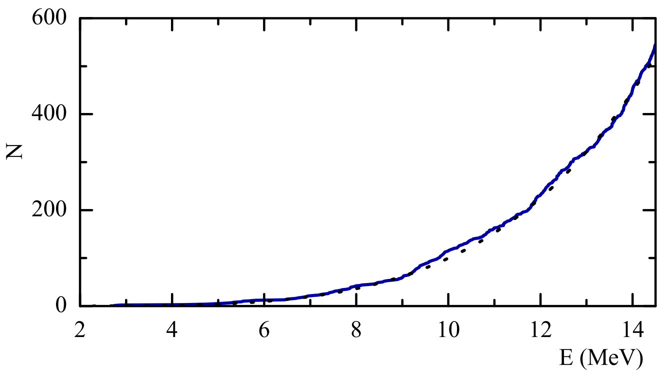

FIG. 4. The staircase function $N(E)$ of the excitation 1^+ energies of ^{130}In calculated with the full two-phonon basis for this work (the solid line). The dotted line denotes the $N(E)$ function obtained with the level density (7).

objects for the study of low-lying $E2$ transitions in its daughter. We consider the electric transitions from five low-energy 1^+ states to the first 3^+ and 2^- excitations and the 1^- ground state of ^{130}In. The calculated excitation energies, the $B(E1)$, $B(E2)$ values, and the partial widths of the 1^+ states are shown in Table I. $B(E1)$ values vary from 10^{-7} to 10^{-4} W.u. The calculated transition probabilities represent important fingerprints for the phonon composition of the 1^+ states. The 1^+_1 wave function of ^{130}In contains a dominant two-phonon configuration $[3^+_1 \otimes 2^+_1]_{\rm QRPA}$ and such a contribution leads to the noticeable $B(E2; 1^+_1 \to 3^+_1)$ value which correlates with the $B(E2; 2^+_1 \to 0^+_{\rm g.s.})$ value of ^{130}Cd. As expected, the $B(E1; 1^+_1 \to 1^-_{\rm g.s.})$ value is negligibly small in our calculation. The 1^+_2 (1^+_4) state exhausts 97% (92%) of the $[3^+_1 \otimes 4^+_1]_{\rm QRPA}$ ($[2^-_1 \otimes 3^-_1]_{\rm QRPA}$) configuration. Therefore, small $B(E1)$ and $B(E2)$ values are obtained. For the 1^+_3 state, the dominance of the one-phonon configuration plays a key role in explaining of the transition probabilities. There is a satisfactory agreement with the $B(E1)$ value in the case of the experimental 1^+_1 state [9], whose theoretical counterpart has a structure dominated by the 2QP configuration $\{\pi 1g_{9/2}, \nu 1g_{7/2}\}$. Also, the experimental branching ratio [9] is well reproduced by our calculation,

$$\frac{\Gamma(E2; 1^+_3 \to 3^+_1)}{\Gamma(E1; 1^+_3 \to 1^-_{\rm g.s.})} = 0.13. \tag{8}$$

This fact indicates that indeed the calculated 1^+_3 state corresponds to the experimental level located at 2120 keV which was also reproduced by the shell model [9]. For the 1^+_5 state, the main contribution to the $B(E2)$ value comes from the configuration $[3^+_1 \otimes 2^+_2]_{\rm QRPA}$, which outweighs the $[3^+_1 \otimes 2^+_1]_{\rm QRPA}$ contribution and results in a noticeable $B(E2)$ value.

It is of importance to investigate if the inclusion of the PPC improves the description of the experimental branching ratio of the γ decay from the 1^+ (2120 keV) state to the 2^-_1 and 1^-_1 states. The 1^-_1 ground state is populated in the experiment [9] nine times less than the 2^-_1 state. As far as we know, neither the shell model nor other microscopic approaches have successfully solved this problem yet. Our calculations give the

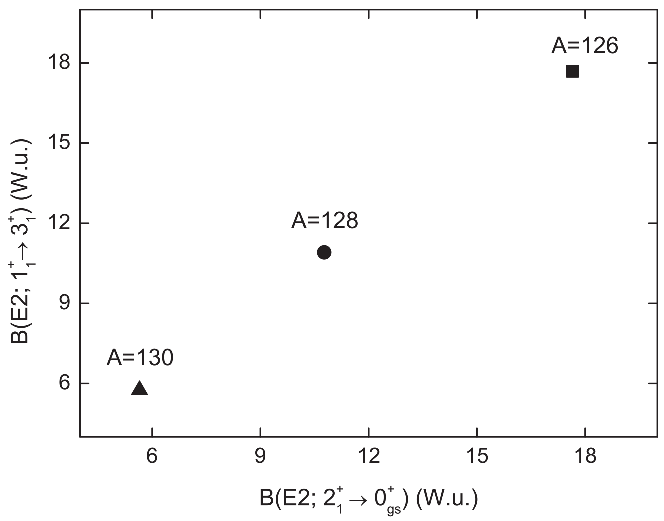

FIG. 5. Comparison of calculated low-lying $E2$ transition strengths in $^{126,128,130}_{\ \ \ \ 49}$In and $^{126,128,130}_{\ \ \ \ 48}$Cd. The calculations take into account the phonon-phonon coupling. $B(E2)$ values are given in Weisskopf units (1 W.u. = $5.94 \times 10^{-2} A^{4/3}\, e^2\, {\rm fm}^4$).

following ratio:

$$\frac{\Gamma(E1; 1^+_3 \to 2^-_1)}{\Gamma(E1; 1^+_3 \to 1^-_{\rm g.s.})} = 1.25. \tag{9}$$

A qualitative description of the experimental data [9] is reached. It is noteworthy that the strong $E3$ transition is also of no help for explaining the puzzling branching ratio,

$$\frac{\Gamma(E3; 1^+_3 \to 2^-_1)}{\Gamma(E1; 1^+_3 \to 1^-_{\rm g.s.})} = 0.003. \tag{10}$$

A possible reason may lie in an underestimation of the $[2^-_1]_{\rm QRPA}$ collectivity and it results in a decrease of the $E1$ transition probability in the case of the Skyrme interaction T43. In any event the present framework allows us to simultaneously describe the basis features of collective excitation spectra both neutral and charge-exchange channels.

V. EXTENSION TO THE $A = 126, 128$ CASES

Using the same set of parameters, we examine the lowest two-phonon 1^+ states of ^{126,128}In populated by the β decay of ^{126,128}Cd. For ^{126,128}In, the spin-parity of the ground state is found to be 3^+. As a result, the first 1^+ state contains a dominant configuration $[3^+_1 \otimes 2^+_1]_{\rm QRPA}$ and such contribution leads to the noticeable $B(E2; 1^+_1 \to 3^+_{\rm g.s.})$ values (see Fig. 5). We find a nice agreement, with $E_x = 0.7$ MeV and $\log ft = 4.1$ for the 1^+ state experimentally identified at 688 keV in ^{126}In [38]. As seen from Fig. 5, there exists a close correlation between the $E22^+_1 \to 0^+_{\rm g.s.}$ and $1^+_1 \to 3^+_1$ transition probabilities of the parent and daughter (respectively) isobaric companions. As proposed in Ref. [39], the 2^+_1 states of ^{126,128,130}Cd are obtained within the PPC calculation, taking into account the Pauli principle corrections. It is worth mentioning that the calculated $B(E2; 2^+_1 \to 0^+_{\rm g.s.})$ value of ^{126}Cd is also in reasonable agreement with the experimental data [40].

VI. SUMMARY AND CONCLUSION

The developed QRPA framework has been applied to β-delayed γ spectroscopy. It is shown that an extension of the phonon space allowing for the additional charge-exchange QRPA excitations substantially enriches the 1^+ spectrum of ^{130}In. An important increase of the level density near the neutron threshold is achieved compared with the case of coupling to the charge-exchange 1^+ phonons and the vibrational 2^+ phonons only [21]. It is shown for the first time that the structure the additional 1^+ states is mostly dominated by the two-phonon configuration built on the charge-exchange 3^+_1 phonon.

The $\{\pi 1g_{9/2}, \nu 1g_{7/2}\}$-dominated 1^+ excitation of ^{130}In was successfully described within the shell model [9]. Our initial motivation was attempting to describe the branching ratio of γ decays and $\log ft$ values for this excitation. Our calculated partial widths and $\log ft$ values are in qualitative agreement with the data. We stress that they represent the first successful comparison between the experimental transition values and those calculated with the Skyrme interaction. We predict the presence of additional two-phonon 1^+ states located below the well-known one-phonon 1^+ state. No experimental counterpart has been identified yet.

The two-phonon configurations are built on the charge-exchange 3^+_1 phonon and the 2^+_1, 4^+_1 phonons. Notice that these states have large $\log ft$ values and small probabilities of the $E1$ transition to the 1^- ground state. Importantly, our results have shown the correlation between the low-lying $E2$ transition strengths of the parent and daughter isobaric companions as compared with the β-decay data of ^{126,128,130}Cd.

For the experimentally well-established one-phonon 1^+ state in ^{130}In, our calculations overestimate the excitation energy and the $B(GT)$ values, which probably points to a particular problem due to the effective interaction rather than to a deficiency of our variational space. The unperturbed $B(GT) = 3.6$ value of the $\{\pi 1g_{9/2}, \nu 1g_{7/2}\}$ state ($\log ft = 3.0$) is too large to be properly renormalized by the inclusion of the QRPA correlation and the two-phonon fragmentation. An additional modification of the Skyrme functional was proposed earlier in order to stabilize the nuclear matter equation of state [41,42]. Our model would probably be improved by including all these ingredients, and comparing them to known experimental data, as done in this work. Nevertheless the existence of two-phonon 1^+ states should be a generic feature of odd-odd nuclei in the vicinity of the doubly magic nucleus ^{132}Sn, and further experimental investigation in this region to check this prediction is probably necessary.

ACKNOWLEDGMENTS

We thank Nguyen Van Giai, Yu.E. Penionzhkevich, H. Sagawa, V.V. Voronov, and V.G. Zelevinsky for useful discussions. This work was supported by the Russian Science Foundation (Grant No. RSF-16-12-10161).

[1] G. Lorusso, S. Nishimura, Z. Y. Xu, A. Jungclaus, Y. Shimizu, G. S. Simpson, P.-A. Söderström, H. Watanabe, F. Browne, P. Doornenbal, G. Gey, H. S. Jung, B. Meyer, T. Sumikama, J. Taprogge, Zs. Vajta, J. Wu, H. Baba, G. Benzoni, K. Y. Chae *et al.*, Phys. Rev. Lett. **114**, 192501 (2015).

[2] K.-L. Kratz, H. Gabelmann, W. Hillebrandt, B. Pfeiffer, K. Schlosser, F.-K. Thielemann, and the ISOLDE collaboration, Z. Phys. A **325**, 489 (1986).

[3] M. Hannawald, V. N. Fedoseyev, U. Köster, K.-L. Kratz, V. I. Mishin, W. F. Mueller, H. L. Ravn, J. Van Roosbroeck, H. Schatz, V. Sebastian, W. B. Walters, and the ISOLDE Collaboration, Nucl. Phys. A **688**, 578c (2001).

[4] I. Dillmann, K.-L. Kratz, A. Wöhr, O. Arndt, B. A. Brown, P. Hoff, M. Hjorth-Jensen, U. Köster, A. N. Ostrowski, B. Pfeiffer, D. Seweryniak, J. Shergur, W. B. Walters, and the ISOLDE Collaboration, Phys. Rev. Lett. **91**, 162503 (2003).

[5] G. Martínez-Pinedo and K. Langanke, Phys. Rev. Lett. **83**, 4502 (1999).

[6] J. J. Cuenca-García, G. Martínez-Pinedo, K. Langanke, F. Nowacki, and I. N. Borzov, Eur. Phys. J. A **34**, 99 (2007).

[7] J. Dobaczewski, I. Hamamoto, W. Nazarewicz, and J. A. Sheikh, Phys. Rev. Lett. **72**, 981 (1994).

[8] L. Coraggio, A. Covello, A. Gargano, N. Itaco, and T. T. S. Kuo, Prog. Part. Nucl. Phys. **62**, 135 (2009).

[9] A. Jungclaus, H. Grawe, S. Nishimura, P. Doornenbal, G. Lorusso, G. S. Simpson, P.-A. Söderström, T. Sumikama, J. Taprogge, Z. Y. Xu, H. Baba, F. Browne, N. Fukuda, R. Gernhäuser, G. Gey, N. Inabe, T. Isobe, H. S. Jung, D. Kameda, G. D. Kim *et al.*, Phys. Rev. C **94**, 024303 (2016).

[10] Evaluated Nuclear Structure Data File, http://www.nndc.bnl.gov/ensdf/ (accessed in March 2019).

[11] I. N. Borzov, Phys. At. Nucl. **79**, 910 (2016).

[12] M. Madurga, R. Surman, I. N. Borzov, R. Grzywacz, K. P. Rykaczewski, C. J. Gross, D. Miller, D. W. Stracener, J. C. Batchelder, N. T. Brewer, L. Cartegni, J. H. Hamilton, J. K. Hwang, S. H. Liu, S. V. Ilyushkin, C. Jost, M. Karny, A. Korgul, W. Królas, A. Kuźniak *et al.*, Phys. Rev. Lett. **109**, 112501 (2012).

[13] V. V. Voronov, D. T. Khoa, and V. Yu. Ponomarev, Bull. Acad. Sci. USSR, Phys. Ser. **48**, 190 (1984).

[14] U. Kneissl, H. H. Pitz, and A. Zilges, Prog. Part. Nucl. Phys. **37**, 349 (1996).

[15] N. Pietralla, Phys. Rev. C **59**, 2941 (1999).

[16] V. G. Soloviev, *Theory of Atomic Nuclei: Quasiparticles and Phonons* (Institute of Physics, Bristol and Philadelphia, 1992).

[17] V. Yu. Ponomarev, Ch. Stoyanov, N. Tsoneva, and M. Grinberg, Nucl. Phys. A **635**, 470 (1998).

[18] V. Yu. Ponomarev, Eur. Phys. J. A **6**, 243 (1999).

[19] N. Auerbach, D. C. Zheng, L. Zamick, and B. A. Brown, Phys. Lett. B **304**, 17 (1993).

[20] V. Zelevinsky, N. Auerbach, and Bui Minh Loc, Phys. Rev. C **96**, 044319 (2017).

[21] A. P. Severyukhin, N. N. Arsenyev, I. N. Borzov, and E. O. Sushenok, Phys. Rev. C **95**, 034314 (2017).

[22] A. P. Severyukhin, V. V. Voronov, I. N. Borzov, N. N. Arsenyev, and Nguyen Van Giai, Phys. Rev. C **90**, 044320 (2014).

[23] Nguyen Van Giai, Ch. Stoyanov, and V. V. Voronov, Phys. Rev. C **57**, 1204 (1998).

[24] A. P. Severyukhin, V. V. Voronov, and N. Van Giai, Prog. Theor. Phys. **128**, 489 (2012).
[25] A. P. Severyukhin and H. Sagawa, Prog. Theor. Exp. Phys. **2013**, 103D03 (2013).
[26] T. Lesinski, M. Bender, K. Bennaceur, T. Duguet, and J. Meyer, Phys. Rev. C **76**, 014312 (2007).
[27] A. P. Severyukhin, V. V. Voronov, and Nguyen Van Giai, Phys. Rev. C **77**, 024322 (2008).
[28] J. Engel, M. Bender, J. Dobaczewski, W. Nazarewicz, and R. Surman, Phys. Rev. C **60**, 014302 (1999).
[29] C. Walz, H. Fujita, A. Krugmann, P. von Neumann-Cosel, N. Pietralla, V. Yu. Ponomarev, A. Scheikh-Obeid, and J. Wambach, Phys. Rev. Lett. **106**, 062501 (2011).
[30] D. Rosiak, M. Seidlitz, P. Reiter, H. Naïdja, Y. Tsunoda, T. Togashi, F. Nowacki, T. Otsuka, G. Colò, K. Arnswald, T. Berry, A. Blazhev, M. J. G. Borge, J. Cederkäll, D. M. Cox, H. De Witte, L. P. Gaffney, C. Henrich, R. Hirsch, M. Huyse *et al.*, Phys. Rev. Lett. **121**, 252501 (2018).
[31] A. P. Severyukhin, V. V. Voronov, and N. Van Giai, Eur. Phys. J. A **22**, 397 (2004).
[32] V. A. Kuzmin and V. G. Soloviev, J. Phys. G: Nucl. Phys. **10**, 1507 (1984).
[33] A. P. Severyukhin, V. V. Voronov, I. N. Borzov, and N. Van Giai, Rom. J. Phys. **58**, 1048 (2013).
[34] G. F. Bertsch and I. Hamamoto, Phys. Rev. C **26**, 1323 (1982).
[35] J. Suhonen, *From Nucleons to Nucleus* (Springer-Verlag, Berlin, 2007).
[36] I. N. Borzov, *Fission and Properties of Neutron-Rich Nuclei*, edited by J. H. Hamilton and A. V. Ramayya (World Scientific, Singapore, 2014), p. 530.
[37] T. Marketin, L. Huther, and G. Martínez-Pinedo, Phys. Rev. C **93**, 025805 (2016).
[38] M. L. Gartner and J. C. Hill, Phys. Rev. C **18**, 1463 (1978).
[39] A. P. Severyukhin, N. N. Arsenyev, N. Pietralla, and V. Werner, Phys. Rev. C **90**, 011306(R) (2014).
[40] S. Ilieva, M. Thürauf, Th. Kröll, R. Krücken, T. Behrens, V. Bildstein, A. Blazhev, S. Bönig, P. A. Butler, J. Cederkäll, T. Davinson, P. Delahaye, J. Diriken, A. Ekström, F. Finke, L. M. Fraile, S. Franchoo, Ch. Fransen, G. Georgiev, R. Gernhäuser *et al.*, Phys. Rev. C **89**, 014313 (2014).
[41] J. Margueron, S. Goriely, M. Grasso, G. Colò, and H. Sagawa, J. Phys. G **36**, 125103 (2009).
[42] J. Margueron and H. Sagawa, J. Phys. G **36**, 125102 (2009).